Quasiclassical nonlinear plasmon resonance in graphene

Jablan, Marinko

Quasiclassical nonlinear plasmon resonance in graphene

Marinko Jablan*
Department of Physics, Faculty of Science, University of Zagreb, 10000 Zagreb, Croatia

(Received 28 October 2019; revised manuscript received 6 February 2020; accepted 11 February 2020; published 27 February 2020)

Electrons in graphene behave like relativistic Dirac particles which can reduce the velocity of light by two orders of magnitude in the form of plasmon-polaritons. Here we show how these properties lead to a peculiar nonlinear plasmon response in the quasiclassical regime of terahertz frequencies. On the one hand, we show how interband plasmon damping is suppressed by the relativistic Klein tunneling effect. On the other hand, we demonstrate huge enhancement of the nonlinear intraband response when the plasmon velocity approaches the resonance with the electron Fermi velocity. This extreme sensitivity to the plasmon intensity could be used for new terahertz technologies.

DOI: 10.1103/PhysRevB.101.085424

I. INTRODUCTION

Nonlinear optics holds promise for the development of ultrafast information processing devices; however, it typically requires huge optical intensities [1]. There is a constant search for new materials with a stronger nonlinear response, so there was naturally huge interest in the nonlinear properties of the recently discovered material graphene [2–30]. Particularly, it was argued that graphene has a strong nonlinear response in the form of interband multiplasmon absorption [12]. However, this is a perturbative process, which, strictly speaking, makes sense only if $N+1$ plasmon absorption is much less than N plasmon absorption. In this paper we wish to discuss what happens at terahertz (THz) frequencies due to many exciting applications in spectroscopy, security, and wireless communications [31]. For such low frequencies, the perturbative approach of multiplasmon absorption breaks down since it gets increasingly harder to distinguish N from $N+1$ plasmon absorption if $N \gg 1$. On the other hand, since then electric field changes extremely slowly in time, the process can be better understood as quasiclassical tunneling. Here we provide a general model that can describe graphene's response to a strong electromagnetic field and solve the model explicitly in the quasiclassical case of slow oscillations in space and time. We are particularly interested in the plasmon-polariton modes which can reduce the velocity of light by two orders of magnitude [32]. We show a huge enhancement of the nonlinear intraband response when the plasmon velocity approaches the resonance with the electron Fermi velocity, while interband plasmon damping is surprisingly suppressed by the Klein tunneling effect [33]. Both effects crucially depend on the massless Dirac Hamiltonian, so we first have to solve the Dirac equation in a strong electromagnetic field. In Sec. II we discuss the quasiclassical approximation, and in Sec. III we discuss interband dynamics beyond the quasiclassical approximation. In Sec. IV we calculate the general nonlinear current response and use this result to analyze interband dissipation in Sec. V and intraband resonance in Sec. VI. Finally, in Sec. VII we provide a discussion and conclusion.

II. QUASICLASSICAL DIRAC STATES IN A STRONG ELECTROMAGNETIC FIELD

Electron motion in graphene is governed by a Dirac Hamiltonian:

$$\hat{H} = v_F \boldsymbol{\sigma} \cdot \hat{\mathbf{p}}, \tag{1}$$

where $v_F = 10^6$ m/s is the Fermi velocity, $\hat{\mathbf{p}} = -i\hbar\nabla$ is the momentum operator, $\boldsymbol{\sigma} = (\sigma_x, \sigma_y)$, and $\sigma_{x,y}$ are Pauli spin matrices [34]. The corresponding eigenstates are

$$\hat{H}\Psi^0_{\mathbf{P}_n} = E_{\mathbf{P}_n}\Psi^0_{\mathbf{P}_n}, \tag{2}$$

$$\Psi^0_{\mathbf{P}_n}(\mathbf{r}, t) = \frac{1}{\sqrt{2L^2}} \begin{pmatrix} e^{-\frac{i}{2}\Phi_{\mathbf{P}_n}} \\ n e^{\frac{i}{2}\Phi_{\mathbf{P}_n}} \end{pmatrix} e^{\frac{i}{\hbar}(\mathbf{P}_n \cdot \mathbf{r} - E_{\mathbf{P}_n} t)}. \tag{3}$$

Here $\mathbf{r} = (x, y)$, L^2 is the area of a graphene flake, the electron momentum is $\mathbf{P}_n = (p_n, p_y)$, and the phase

$$e^{i\Phi_{\mathbf{P}_n}} = \frac{p_n + ip_y}{|\mathbf{P}_n|}. \tag{4}$$

Note that electron energies (eigenvalues) show a peculiar linear dispersion:

$$E_{\mathbf{P}_n} = n v_F |\mathbf{P}_n|, \tag{5}$$

where $n = -1$ represents the valence band and $n = 1$ represents the conduction band.

To describe the behavior of graphene in an external vector potential $\mathbf{A}(\mathbf{r}, t)$ we need to solve the Dirac equation:

$$i\hbar \frac{\partial \Psi}{\partial t} = v_F \boldsymbol{\sigma} \cdot (\hat{\mathbf{p}} - e\mathbf{A})\Psi. \tag{6}$$

Particularly, we are interested in the longitudinal field:

$$\mathbf{A}(\mathbf{r}, t) = \mathbf{e}_x A(\mathbf{r}, t) = \mathbf{e}_x A_0 \sin u, \tag{7}$$

where $u = \omega t - qx$ and $\mathbf{e}_x$ is the unit vector in the x direction. This field can then describe plasmon-polariton modes whose

*mjablan@phy.hr

velocity is much smaller than the speed of light $\omega/q \ll c$ [32]. The case of Dirac particles in the transverse field at the light line $\omega = qc$ was solved by Volkov [35], but unfortunately, this approach does not work in our case. On the other hand, since we are primarily interested in slow oscillations in space and time, we can search for a solution in the form of the quasiclassical state:

$$\Psi^{qc} = ae^{\frac{i}{\hbar}S}, \tag{8}$$

where S is the classical action and a is the slowly varying amplitude [36]. Moreover, we will see that these states enable us to get a much more general description of the system, including the fast oscillations in space and time. As a lowest approximation, let us insert this ansatz into the Dirac equation and neglect terms containing $\hbar$, which is an excellent approximation in the case of slow oscillations, i.e., for $\hbar\omega \ll E_F$ and $\hbar q \ll p_F$, where E_F is the Fermi energy and $p_F = E_F/v_F$ is the Fermi momentum. We obtain the equation of motion,

$$-\frac{\partial S}{\partial t}a = v_F\boldsymbol{\sigma}\cdot(\nabla S - e\mathbf{A})a, \tag{9}$$

which is solved with the following quasiclassical states:

$$\Psi^{qc}_{\mathbf{P}_n}(\mathbf{r},t) = \frac{1}{\sqrt{2L^2}}\begin{pmatrix} e^{-\frac{i}{2}\Phi_{\mathbf{P}^c_n - e\mathbf{A}}} \\ ne^{\frac{i}{2}\Phi_{\mathbf{P}^c_n - e\mathbf{A}}}\end{pmatrix} e^{\frac{i}{\hbar}S_{\mathbf{P}_n}}, \tag{10}$$

where $S_{\mathbf{P}_n}$ satisfies the Hamilton-Jacobi equation for the classical action of the Dirac particle,

$$\frac{\partial S_{\mathbf{P}_n}}{\partial t} = -nv_F\left|\nabla S_{\mathbf{P}_n} - e\mathbf{A}\right|, \tag{11}$$

and we have introduced the classical momentum $\mathbf{P}^c_n = \nabla S_{\mathbf{P}_n}$ [37]. Since y is a cyclic variable, the momentum is conserved in the y direction, and we can write $\mathbf{P}^c_n = (p^c_n, p_y)$, where $p^c_n = \partial S_{\mathbf{P}_n}/\partial x$. The phase is defined as

$$e^{i\Phi_{\mathbf{P}^c_n - e\mathbf{A}}} = \frac{p^c_n - eA + ip_y}{\left|\mathbf{P}^c_n - e\mathbf{A}\right|}. \tag{12}$$

We assume that the field is slowly turned on:

$$A(\mathbf{r},t) = A_0\sin(\omega t - qx)e^{\eta t}, \tag{13}$$

where $\eta \ll \omega$, so that our quasiclassical state (10) adiabatically evolves from the free particle state (3); that is, we set the initial condition to be

$$\Psi^{qc}_{\mathbf{P}_n}(\mathbf{r}, t=-\infty) = \Psi^0_{\mathbf{P}_n}(\mathbf{r},t). \tag{14}$$

To solve the Hamilton-Jacobi equation we use the ansatz [38]

$$S_{\mathbf{P}_n}(\mathbf{r},t) = \mathbf{P}_n\cdot\mathbf{r} - E_{\mathbf{P}_n}t + F_{\mathbf{P}_n}(u), \tag{15}$$

which gives the following equation for the unknown function $\dot{F} = \frac{dF}{du}$:

$$-E_{\mathbf{P}_n} + \omega\dot{F}_{\mathbf{P}_n} = -nv_F\sqrt{\left(p_n - q\dot{F}_{\mathbf{P}_n} - eA\right)^2 + p_y^2}. \tag{16}$$

It is simple to solve this quadratic equation and obtain the classical momentum and energy,

$$p^c_n = \frac{\partial S_{\mathbf{P}_n}}{\partial x} = p_n - q\dot{F}_{\mathbf{P}_n}, \tag{17}$$

$$E^c_{\mathbf{P}_n} = -\frac{\partial S_{\mathbf{P}_n}}{\partial t} = E_{\mathbf{P}_n} - \omega\dot{F}_{\mathbf{P}_n}, \tag{18}$$

explicitly as

$$p^c_n - eA = \frac{1}{1-\frac{q^2v_F^2}{\omega^2}}\left(p_n - \frac{q}{\omega}E_{\mathbf{P}_n} - eA + n\frac{qv_F}{\omega}\sqrt{\left(p_n - \frac{q}{\omega}E_{\mathbf{P}_n} - eA\right)^2 + p_y^2\left(1-\frac{q^2v_F^2}{\omega^2}\right)}\right) \tag{19}$$

and

$$E^c_{\mathbf{P}_n} = \frac{v_F}{1-\frac{q^2v_F^2}{\omega^2}}\left(\frac{qv_F}{\omega}\left(p_n - \frac{q}{\omega}E_{\mathbf{P}_n} - eA\right) + n\sqrt{\left(p_n - \frac{q}{\omega}E_{\mathbf{P}_n} - eA\right)^2 + p_y^2\left(1-\frac{q^2v_F^2}{\omega^2}\right)}\right). \tag{20}$$

To check that, initially, $p^c_n = p_n$ and $E^c_{\mathbf{P}_n} = E_{\mathbf{P}_n}$, one can note that $A(\mathbf{r}, t=-\infty) = 0$ and use the following identity:

$$\sqrt{\left(p_n - \frac{q}{\omega}E_{\mathbf{P}_n}\right)^2 + p_y^2\left(1-\frac{q^2v_F^2}{\omega^2}\right)} = n\left(\frac{E_{\mathbf{P}_n}}{v_F} - \frac{qv_F}{\omega}p_n\right). \tag{21}$$

Finally, by using Eqs. (15) and (18) it is convenient to write the action implicitly as

$$S_{\mathbf{P}_n} = \left(p_n - \frac{q}{\omega}E_{\mathbf{P}_n}\right)x + p_y y - \frac{1}{\omega}\int_0^u E^c_{\mathbf{P}_n}du. \tag{22}$$

III. INTERBAND DYNAMICS BEYOND THE QUASICLASSICAL APPROXIMATION

We can, however, get a much more general description of the system using the quasiclassical states (10). Let us start with some general wave packet of the form

$$\Psi(\mathbf{r},t) = \sum_{n\mathbf{P}_n} c_{\mathbf{P}_n}(u)\Psi^{qc}_{\mathbf{P}_n}(\mathbf{r},t) \tag{23}$$

and insert it into the Dirac equation. It is then most convenient to consider the triplet $\{x, y, u\}$ independent variables since $\{x, y\}$ variables appear only in the exponent $e^{\frac{i}{\hbar}S_{\mathbf{P}_n}}$. From Eq. (22) we then see that our system dynamics can couple states $\mathbf{P}_n$ and $\mathbf{P}'_n$ only if $p'_y = p_y$ and $p'_n - \frac{q}{\omega}E_{\mathbf{P}'_n} = p_n - \frac{q}{\omega}E_{\mathbf{P}_n}$. The first condition is just the conservation of momentum in the y direction, while the second condition corresponds to the multiphoton absorption process [12] which is given by the conservation of momentum, $p'_n - p_n = N\hbar q$, and conservation of energy, $E_{\mathbf{P}'_n} - E_{\mathbf{P}_n} = N\hbar\omega$. In this paper we consider only the case $qv_F/\omega < 1$ since, otherwise, the (intraband) single-photon absorption dominates the system response [12,32]. In this case it is straightforward to show that multiphoton absorption can couple only states in different bands $n' = -n$; that is, the second condition gives

$$p_{-n} - \frac{q}{\omega}E_{\mathbf{P}_{-n}} = p_n - \frac{q}{\omega}E_{\mathbf{P}_n}, \tag{24}$$

which can be solved as

$$p_{-n} = \frac{p_n\left(1+\frac{q^2v_F^2}{\omega^2}\right) - 2\frac{q}{\omega}E_{\mathbf{P}_n}}{1-\frac{q^2v_F^2}{\omega^2}}. \tag{25}$$

It is also convenient to calculate the density of states:

$$\frac{dp_{-n}}{dp_n} = -\frac{E_{\mathbf{P}_{-n}}}{E_{\mathbf{P}_n}}. \tag{26}$$

We see now that within our general wave packet, states $\sum_n c_{\mathbf{P}_n}\Psi^{qc}_{\mathbf{P}_n}$ evolve completely independently from one another. Let us then focus on the state

$$\Psi_{\mathbf{P}_m}(\mathbf{r},t) = \sum_{n=\pm m} c_{\mathbf{P}_n}(u)\Psi^{qc}_{\mathbf{P}_n}(\mathbf{r},t), \tag{27}$$

subject to the initial condition

$$\Psi_{\mathbf{P}_m}(\mathbf{r},t=-\infty) = \Psi^0_{\mathbf{P}_m}(\mathbf{r},t), \tag{28}$$

i.e.,

$$c_{\mathbf{P}_m}(u=-\infty) = 1, \tag{29}$$

$$c_{\mathbf{P}_{-m}}(u=-\infty) = 0. \tag{30}$$

We can further simplify calculations by writing the state in a more general form:

$$\Psi_{\mathbf{P}_m}(\mathbf{r},t) = \sum_{n=\pm m} c_{\mathbf{P}_n}(u)b_{\mathbf{P}_n}(u)\Psi^{qc}_{\mathbf{P}_n}(\mathbf{r},t), \tag{31}$$

where we have introduced additional functions $b_{\mathbf{P}_n}(u)$ subject to the initial condition,

$$b_{\mathbf{P}_m}(u=-\infty) = 1. \tag{32}$$

Particularly, by choosing

$$b_{\mathbf{P}_n}(u) = B_{\mathbf{P}_n}\sqrt{E^c_{\mathbf{P}_n}/\Delta E^c_{\mathbf{P}_n}}, \tag{33}$$

where $\Delta E^c_{\mathbf{P}_n} = E^c_{\mathbf{P}_n} - E^c_{\mathbf{P}_{-n}}$ and

$$B_{\mathbf{P}_m} = B_{\mathbf{P}_{-m}} = \sqrt{\Delta E_{\mathbf{P}_m}/E_{\mathbf{P}_m}}, \tag{34}$$

we obtain (see Appendix A)

$$\left|c_{\mathbf{P}_m}(u)\right|^2 + \left|c_{\mathbf{P}_{-m}}(u)\right|^2 = 1. \tag{35}$$

We can then interpret $|c_{\mathbf{P}_n}(u)|^2$ as the probability of finding the electron in band n as a function of u. However, one needs to be careful about this interpretation since $u = \omega t - qx$, so this is not the standard probability as a function of time t. Finally, in the case of slow oscillations in space and time we can use the Landau-Zener model [36] to obtain explicitly

$$|c_{-m}(u=\infty)|^2 = \exp\left(\frac{1}{\hbar\omega}\mathrm{Im}\int_C \Delta E^c_m du\right) = K, \tag{36}$$

where the integration contour C goes around the complex transition point u_0 which is given by $\Delta E^c_m(u_0) = 0$. Here K is the transition probability for a single passage, while the probability for a double passage is $2K(1-K)$ [36] (see also Appendix D).

IV. NONLINEAR CURRENT RESPONSE

To describe the general case of a mixed state we can introduce the density matrix

$$\rho(\mathbf{r},t,\mathbf{r}',t') = 4\sum_{n\mathbf{P}_n} f_{\mathbf{P}_n}\Psi^*_{\mathbf{P}_n}(\mathbf{r}',t')\Psi_{\mathbf{P}_n}(\mathbf{r},t), \tag{37}$$

where $f_{\mathbf{P}_n} = \frac{1}{e^{(E_{\mathbf{P}_n}-E_F)/kT}+1}$ is the Fermi-Dirac distribution at temperature T [39] and we took into account two-spin and two-valley degeneracy in graphene [34]. We can then write the induced current as [36]

$$\mathbf{j}(\mathbf{r},t) = \int d\mathbf{R}[\hat{\mathbf{j}}(\mathbf{r})\rho(\mathbf{R},t,\mathbf{R}',t)]_{\mathbf{R}'=\mathbf{R}}, \tag{38}$$

where $\hat{\mathbf{j}}(\mathbf{r}) = ev_F\boldsymbol{\sigma}\delta(\hat{\mathbf{r}}-\mathbf{r})$ is the current density operator of graphene [34]. Since $j_y = 0$ due to symmetry, we can focus only on the x component:

$$j_x(\mathbf{r},t) = \frac{4}{L^2}\sum_{n\mathbf{P}_n} f_{\mathbf{P}_n}\Bigg[\left|c_{\mathbf{P}_n}\right|^2 b^2_{\mathbf{P}_n}ev^c_{\mathbf{P}_n} + \left|c_{\mathbf{P}_n\mathbf{P}_{-n}}\right|^2 b^2_{\mathbf{P}_n\mathbf{P}_{-n}}ev^c_{\mathbf{P}_{-n}} + \frac{\Delta E^c_{\mathbf{P}_n}}{\dot{A}}\frac{B^2_{\mathbf{P}_n}}{2}\left(1-\frac{q^2v_F^2}{\omega^2}\right)\frac{d\left|c_{\mathbf{P}_n\mathbf{P}_{-n}}\right|^2}{du}\Bigg], \tag{39}$$

where $\dot{A} = \frac{dA}{du}$ and $v^c_{\mathbf{P}_n} = \frac{\partial E^c_{\mathbf{P}_n}}{\partial p^c_n} = nv_F\cos\Phi_{\mathbf{P}^c_n - e\mathbf{A}}$ is the x component of the classical velocity (see Appendix B). We can consider that the state with initial conditions $c_{\mathbf{P}_n} = 1$ and $c_{\mathbf{P}_n\mathbf{P}_{-n}} = 0$ evolves independently from the state with initial conditions $c_{\mathbf{P}_{-n}} = 1$ and $c_{\mathbf{P}_{-n}\mathbf{P}_n} = 0$, after averaging over thermally randomized initial phases. We can now interpret the first part of Eq. (39) ($|c_n|^2 b_n^2 ev_n^c$) as the current of the electrons that have stayed in their original band and the second part as the current of the electrons that have jumped into different band, while the third part describes the actual interband transition process, i.e., the energy dissipation. Note that we could choose $b_{\mathbf{P}_n} = 1$, but in that case it is no longer true that $|c_{\mathbf{P}_n}|^2 + |c_{\mathbf{P}_n\mathbf{P}_{-n}}|^2 = 1$, and the interband part becomes much more complicated.

V. INTERBAND DISSIPATED POWER

While Eq. (39) is exact, it requires numerical evaluation of coefficients $c_{\mathbf{P}_n}(u)$ [see Eq. (A8)]. However, in the case of slow oscillations in space and time we can use the Landau-Zener model (36). Let us first find the dissipated power $P = \int d\mathbf{r}\,\mathbf{j}\cdot\mathbf{E} = \int d\mathbf{r}\,j_xE_x$, where $E_x = -\frac{\partial A_x}{\partial t} = -\omega\dot{A}$. Since $\dot{A} = A_0\cos u$, only the third interband part contributes to the dissipation:

$$P = 4\sum_{\mathbf{P}_1}\left(f_{\mathbf{P}_{-1}} - f_{\mathbf{P}_1}\right)\frac{\left[\Delta E^c_{\mathbf{P}_1}(u)\right]_{\min}}{T} \times 2K(1-K)\frac{B^2_{\mathbf{P}_1}}{2}\left(1-\frac{q^2v_F^2}{\omega^2}\right). \tag{40}$$

Here we have used the following relation:

$$\frac{dp_{-n}}{dp_n}\frac{B^2_{\mathbf{P}_{-n}}}{B^2_{\mathbf{P}_n}} = -\frac{dp_{-n}}{dp_n}\frac{E_{\mathbf{P}_n}}{E_{\mathbf{P}_{-n}}} = 1, \tag{41}$$

which is a direct consequence of Eq. (26). Also, we used

$$\frac{d\left|c_{\mathbf{P}_n\mathbf{P}_{-n}}\right|^2}{du} = 2K(1-K)\delta(u-\xi); \tag{42}$$

that is, we assumed that the transition happens at a real point ξ when the gap is minimal, $\Delta E^c_{\mathbf{P}_1}(\xi) = [\Delta E^c_{\mathbf{P}_1}(u)]_{\min}$, since then tunneling probability is largest (see also Appendix D). We can now clearly see a physical interpretation of every part of Eq. (40): $f_{-1} - f_1$ is the Pauli principle, $[\Delta E^c_1]_{\min}$ is the dissipated energy per oscillation period $T = 2\pi/\omega$, and $2K(1-K)\frac{B_1^2}{2}(1-\frac{q^2v_F^2}{\omega^2})$ is the transition probability. As we noted, $|c_n(u)|^2$ is not the actual probability at time t since $u = \omega t - qx$. Only in the case of homogenous field, $q = 0$, do we get that K $[2K(1-K)]$ is the transition probability in time for a single passage (double passage). Note that K from Eq. (36) exponentially decreases as we increase the gap $[\Delta E^c_1]_{\min}$. The leading contribution to the dissipated power then comes from the states near the lowest gap (minimum of $[\Delta E^c_1]_{\min}$), i.e., for $p_y = 0$ and $p_1 = p_F$, since the Pauli principle requires that $p_1^2 + p_y^2 \geqslant p_F^2$ for $kT \ll E_F$. In that case,

$$\left[\Delta E^c_1\right]_{\min} = \frac{2v_F\left|p_F\left(1-\frac{qv_F}{\omega}\right) - eA_0\right|}{1-\frac{q^2v_F^2}{\omega^2}}, \tag{43}$$

and we see that at the threshold $A_0 = A_{nl}$, where

$$A_{nl} = \left(1-\frac{qv_F}{\omega}\right)\frac{p_F}{e}, \tag{44}$$

the gap disappears $[\Delta E^c_1]_{\min} = 0$, and we get a perfect tunneling $K = 1$ for the single passage (just like the Klein tunneling effect [33]). However, the particle simply returns back to the original band upon the return passage since $2K(1-K) = 0$. In other words we expect to see P grow exponentially with A_0 until the threshold A_{nl}, when it starts to saturate. Finally, since Klein tunneling does not result in energy dissipation ($[\Delta E^c_1]_{\min} = 0$), we get very small values for the total dissipated power [see Fig. 1(b)]. We could also calculate dissipated power by a Keldysh approach [40]; however, one has to specially deal with the closely spaced singularities at the onset of Klein tunneling.

VI. INTRABAND NONLINEAR RESONANCE

With the aforementioned analysis in mind we can find the dominant contribution to the current (39) by writing $|c_{\mathbf{P}_n}| \approx 1$ and $|c_{\mathbf{P}_n\mathbf{P}_{-n}}| \approx 0$, so that $j_x(\mathbf{r},t) = \frac{4}{L^2}\sum_{n\mathbf{P}_n} f_{\mathbf{P}_n} b^2_{\mathbf{P}_n} e v^c_{\mathbf{P}_n}$. If we then assume that $kT \ll E_F$ so that the valence band is completely occupied (and thus cannot conduct electricity), we are left with the conduction band ($n = 1$) current, which can be written as (see Appendix B)

$$j_x = \frac{4e}{h^2}\int dp_1 dp_y\, f_1 \frac{\partial E^c_1}{\partial p_1} = -\frac{4e}{h^2}\int dp_1 dp_y \frac{\partial f_1}{\partial p_1} E^c_1. \tag{45}$$

Current (45) is plotted in Fig. 1(c) for the local case $qv_F/\omega \approx 0$ and in Fig. 1(d) for the nonlocal case $qv_F/\omega \approx 1$. In the local case it is easy to visualize the result since the field uniformly shifts all electrons in momentum space: $p_1 \to p_1 - eA_0 \sin\omega t$ [see the inset in Fig. 1(c)]. Then due to peculiar

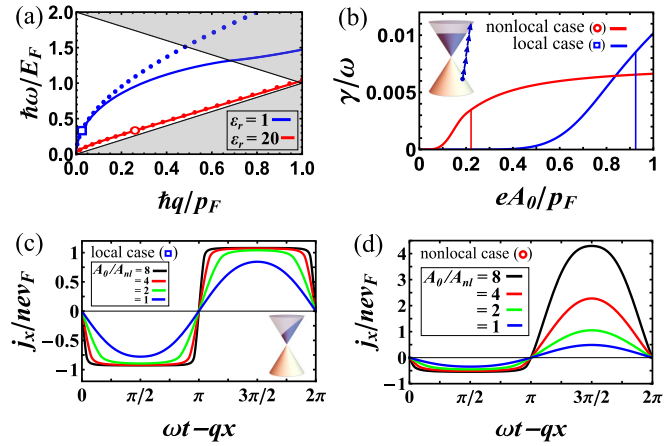

FIG. 1. (a) Plasmon dispersion in graphene for different dielectric environments ε_r. Solid lines: Random-phase approximation [32]. Dots: quasiclassical linear response from Eq. (C4). Gray area: regime of single-plasmon absorption, i.e., linear Landau damping. The open square represents a point for which $qv_F/\omega \approx 0.08$ and local theory is applicable. The nonlinear response for this point is shown in (b) and (c). The open circle represents the nonlocal case $qv_F/\omega \approx 0.8$, for which the nonlinear response is shown in (b) and (d). (b) Quasiclassical nonlinear Landau damping: dependence of the plasmon linewidth on the amplitude of the vector potential A_0. The vertical line represents the amplitude $A_0 = A_{nl} = (1-qv_F/\omega)p_F/e$ and the onset of the Klein tunneling. The inset shows the multiplasmon absorption process, which for low frequencies $\hbar\omega \ll 2E_F$ is better described as a quasiclassical Landau-Zener tunneling. (c) Intraband current response at different amplitudes A_0 for the local case. The inset shows a snapshot of the electron dynamics. (d) Intraband nonlocal current response.

linear Dirac dispersion, at the peak field for $eA_0 \gg p_F$ the majority of electrons reach the maximum electron velocity v_F in graphene, and the current saturates. While some of these intraband effects were discussed for the local case [3,16], we show a peculiar physics in the nonlocal response. Particularly, for $qv_F/\omega \approx 1$ the current becomes extremely nonlinear since classical energy (20) is very asymmetric depending on the sign of the field: $E^c_1 \propto \Theta(p_1 - \sqrt{p_1^2 + p_y^2} - eA)$. Particularly for $eA > 0$ very little current flows compared to the $eA < 0$ case, and our system behaves like a rectifier [see Fig. 1(d)]. Reaching this nonlinear response requires only that $(p_1 - \frac{q}{\omega}E_{\mathbf{P}_1} - eA)^2 \gg p_y^2(1-\frac{q^2v_F^2}{\omega^2})$. For $qv_F/\omega \approx 1$ this will be satisfied almost always if $eA_0 \gg eA_{nl} = (1-qv_F/\omega)p_F$ (see Appendix C for the linear response regime $eA_0 \ll eA_{nl}$). Figures 1(c) and 1(d) show the case of the photon energy $\hbar\omega \approx E_F/3$, which for an electron concentration $n = \frac{p_F^2}{\pi\hbar^2} = 10^{12}\,\mathrm{cm}^{-2}$ corresponds to the frequency $\frac{\omega}{2\pi} \approx 9\,\mathrm{THz}$. At room temperature, $kT \approx 0.2\,E_F$, so we can neglect temperature effects. Note that the threshold for the onset of nonlinear behavior, $A_{nl} = (1-qv_F/\omega)p_F/e$, decreases linearly with Fermi energy like in the local case [3,16]. But what is especially intriguing is that A_{nl} goes to zero at the resonance of plasmon velocity and the electron Fermi velocity in graphene, dramatically enhancing the nonlinear response in the nonlocal case. This extreme sensitivity to the electric field amplitude and the rectifying effect shown in Fig. 1(d) could be used for

the detection of THz radiation and, in more advanced applications, for information processing devices [1]. Of course, like in atomic resonances, the final scale of nonlinearity will be determined by the loss mechanisms. Graphene room temperature DC mobility can be larger than $\mu = 10\ \mathrm{m}^2/\mathrm{V\,s}$ [41,42], which corresponds to damping rate $\gamma = \frac{ev_F^2}{\mu E_F} \approx 0.9$ THz (see Appendix C). Since $\hbar\omega \sim kT$, this will not be drastically changed at THz frequencies. The system response is then undetermined within the linewidth $\gamma/\omega \approx 0.01$, so for $1 - qv_F/\omega < 0.01$ this theory has to be supplemented by taking losses into account.

VII. DISCUSSION AND CONCLUSION

For small fields $eA_0 \ll eA_{nl}$ we can linearize the current (45) to obtain $j_x = i\omega\sigma(q,\omega)A$. However, oscillating current will also induce a vector potential that will act back on the current. If we then introduce some external potential A^{ext}, the current will respond not only to A^{ext} but to the total self-consistent potential A of the amplitude $A_0 = \frac{A_0^{\mathrm{ext}}}{1+\frac{i\sigma(q,\omega)}{\omega 2\varepsilon_0\varepsilon_r}}$ (see Appendix C). One can see that it is possible to have self-sustained oscillations of the electron gas (plasmon-polaritons) even in the absence of the external field if $1 + \frac{iq\sigma(q,\omega)}{\omega 2\varepsilon_0\varepsilon_r} = 0$, with the corresponding plasmon dispersion $\omega(q)$ plotted in Fig. 1(a). Furthermore, we see that we get a huge enhancement of the external field at the plasmon resonance. Note that this analysis gets much more complicated for large fields $eA_0 \gg eA_{nl}$ since the current response is extremely nonlinear and it will produce a vector potential with many new harmonics [see Figs. 1(c) and 1(d)], while our calculation is based on the single harmonic in the vector potential $A = A_0 \sin(\omega t - qx)$. The precise analysis including the full self-consistent nonlinear effects simply goes beyond the scope of this paper, and here we can discuss only some qualitative properties. The generation of direct current or higher harmonics, which all extract energy from the basic harmonic, would manifest as effective plasmon damping. Therefore, one would see an increase in the plasmon linewidth due to pure intraband effects in addition to the interband dissipation process. There would also be an intensity-dependent response at the basic harmonic which would shift the plasmon dispersion. Yet an especially interesting case occurs for large ε_r when both the plasmon dispersion and higher harmonics lie close to the line $\omega = qv_F$ since then self-consistent effects would additionally enhance higher harmonics. It is interesting to note that in that case all harmonics separately will show similar behavior with a similar threshold field $eA_{nl} = (1 - qv_F/\omega)p_F$, but a particularly strong nonlinear interaction between these harmonics might occur. On the other hand, to test the quantitative predictions of this work for large fields $eA_0 \gg eA_{nl}$ it would be simplest to measure the DC component of the current (45) for nonlocal excitation $\omega \gtrsim qv_F$, making sure that none of the harmonics cuts the plasmon dispersion.

To quantify interband plasmon dissipation it is simplest to look at the dissipation rate $\gamma = P/W$, where W is the total plasmon energy. The energy density of a dispersive medium can be written as [43] $u = \frac{1}{2}\mathrm{Re}\frac{d(\omega\varepsilon)}{d\omega}\langle \mathbf{E}^2\rangle$, which in the case of graphene plasmons gives [12]

$$\frac{W}{L^2} = \frac{A_0^2\omega^3}{4}\frac{d}{d\omega}\left(\frac{-\mathrm{Im}\sigma(q,\omega)}{\omega}\right). \tag{46}$$

One can then write the plasmon linewidth as $\gamma/\omega = P/\omega W$, which basically says what fraction of the plasmon energy is dissipated during a single oscillation period. While plasmon linewidth is very small, it can be, nonetheless, detected in precise measurements due to very specific dependence on the plasmon amplitude A_0. For small amplitudes we see exponential growth with A_0 typical of the quasiclassical tunneling, while for large amplitudes we see the saturation effect, which signals the onset of Klein tunneling [Fig. 1(b)]. We call this effect quasiclassical nonlinear Landau damping to distinguish it from the nonlinear Landau damping discussed recently in classical plasma at high frequencies [44]. Note that expression (40) does not represent truly dissipated energy, but more like a stored energy that can be retrieved back from the system. One spectacular way in which this can happen is if, after the electron has tunneled into a different band, it gets accelerated by this strong electric field and finally recombines with the hole it left behind, liberating this huge energy from the field in the form of a train of high harmonics [45,46]. While this too is a very weak effect, it shows intriguing properties in the frequency space. Namely, this train of harmonics adds up to a pulse extremely localized in time on the order of attoseconds [47], an effect that would be even more interesting with plasmons in graphene due to their subwavelength nature [32] since the resulting pulse would be localized in time and space. While high-harmonic generation with plasmons in graphene was analyzed numerically [19], our quasiclassical states offer the most natural platform to take into account the quasiclassical nature of this problem [46].

In conclusion we have developed a general model that can treat the response of graphene to a strong electromagnetic field, which we explicitly solved in the quasiclassical regime of THz frequencies. Interband transitions were analyzed via the Landau-Zener model, leading to plasmon dissipation which is, however, suppressed by the Klein tunneling effect. Moreover, our quasiclassical states could be further used to find how this dissipated energy can be extracted back via the three-step process of high-harmonic generation [45–47]. Most notably, we demonstrated a huge enhancement of the nonlinear intraband response near the resonance of the plasmon velocity and electron Fermi velocity in graphene. This extreme sensitivity to the plasmon intensity could be used for nonlinear, subwavelength THz technologies like detectors and information processing devices.

ACKNOWLEDGMENTS

This work was supported by the University of Zagreb (Research Support No. 20283205) and the QuantiXLie Centre of Excellence, a project cofinanced by the Croatian government and European Union through the European Regional Development Fund–the Competitiveness and Cohesion Operational Programme (Grant No. KK.01.1.1.01.0004).

APPENDIX A: INTERBAND DYNAMICS BEYOND THE QUASICLASSICAL APPROXIMATION

To simplify notation let us write our state $\Psi_{\mathbf{P}_m}(\mathbf{r},t) = \sum_n c_{\mathbf{P}_n}(u) b_{\mathbf{P}_n}(u) \Psi^{qc}_{\mathbf{P}_n}(\mathbf{r},t)$ as

$$\Psi_m = \sum_{n=\pm m} c_n b_n a_n e^{\frac{i}{\hbar}S_n}, \tag{A1}$$

where we have used $\Psi^{qc}_n(\mathbf{r},t) = a_n(u) e^{\frac{i}{\hbar}S_n}$. We use this ansatz to solve the Dirac equation $i\hbar\frac{\partial\Psi}{\partial t} = v_F\boldsymbol{\sigma}\cdot(\hat{\mathbf{p}} - e\mathbf{A})\Psi$. By choosing a_n, S_n to satisfy the quasiclassical equation of motion $-\frac{\partial S_n}{\partial t}a_n = v_F\boldsymbol{\sigma}\cdot(\nabla S_n - e\mathbf{A})a_n$, we obtain the equation for the remaining unknowns: $(\omega - q v_F\sigma_x)\sum_n \frac{d}{du}(c_n b_n a_n)e^{\frac{i}{\hbar}S_n} = 0$. Since the matrix

$$M = \omega - q v_F\sigma_x = \begin{pmatrix} \omega & -q v_F \\ -q v_F & \omega \end{pmatrix} \tag{A2}$$

is invertible for $\omega \neq q v_F$, we multiply the previous equation by M^{-1} to obtain the (exact) evolution equation:

$$\sum_n \frac{d}{du}(c_n b_n a_n)e^{\frac{i}{\hbar}S_n} = 0. \tag{A3}$$

We can enormously simplify further calculations by choosing the function $b_n(u)$ so that $\frac{d(b_n a_n)}{du} \propto b_{-n}a_{-n}$, which means that we maximally decouple dynamics between the bands. It is easy to solve this equation via the substitution $b_n = e^{\beta_n}$ to obtain $b_n(u) = B_n\sqrt{E^c_n/\Delta E^c_n}$, and here we give a short check of the solution. Let us focus on a spinor,

$$d_n = b_n a_n = \frac{B_n}{\sqrt{2L^2}}\sqrt{\frac{E^c_n}{\Delta E^c_n}}\begin{pmatrix} e^{-\frac{i}{2}\Phi_{\mathbf{P}^c_n - e\mathbf{A}}} \\ n e^{\frac{i}{2}\Phi_{\mathbf{P}^c_n - e\mathbf{A}}} \end{pmatrix}. \tag{A4}$$

Then since $E^c_n = n v_F\sqrt{(p^c_n - eA)^2 + p_y^2}$, we can write $e^{i\Phi_{\mathbf{P}^c_n - e\mathbf{A}}} = (p^c_n - eA + ip_y)n v_F/E^c_n$ and

$$\begin{aligned} d_n &= \frac{B_n}{\sqrt{2L^2}}\sqrt{\frac{v_F}{n\Delta E^c_n}}\begin{pmatrix} \sqrt{p^c_n - eA - ip_y} \\ n\sqrt{p^c_n - eA + ip_y} \end{pmatrix} \\ &= \frac{B_n}{\sqrt{2L^2}}\begin{pmatrix} D_n \\ n D^*_n \end{pmatrix}. \end{aligned} \tag{A5}$$

Here we have used the fact that nE^c_n and $n\Delta E^c_n$ are positive quantities, and we have introduced the function

$$D_n = \sqrt{\frac{p_n - \frac{q}{\omega}E_n - eA - ip_y\left(1 - \frac{q^2v_F^2}{\omega^2}\right)}{2\sqrt{\left(p_n - \frac{q}{\omega}E_n - eA\right)^2 + p_y^2\left(1 - \frac{q^2v_F^2}{\omega^2}\right)}} + n\frac{q v_F}{\omega}}. \tag{A6}$$

If we then choose $B_{-m} = B_m = \text{const}$, it is straightforward to show that

$$\begin{aligned} \dot{d}_n &= d_{-n}\frac{-\frac{i}{2}p_y e\dot{A}\sqrt{1 - \frac{q^2v_F^2}{\omega^2}}}{\left(p_n - \frac{q}{\omega}E_n - eA\right)^2 + p_y^2\left(1 - \frac{q^2v_F^2}{\omega^2}\right)} \\ &= d_{-n}\frac{-2iv_F^2 p_y e\dot{A}}{\left(\Delta E^c_n\right)^2}\left(1 - \frac{q^2v_F^2}{\omega^2}\right)^{-3/2}. \end{aligned} \tag{A7}$$

If we now insert this expression into the evolution Eq. (A3), $\sum_n (\dot{c}_n d_n + c_n\dot{d}_n)e^{\frac{i}{\hbar}S_n} = 0$, we obtain the following relations for the coefficients $c_n(u)$:

$$\dot{c}_{-n} = i c_n e^{\frac{i}{\hbar}(S_n - S_{-n})}\frac{2v_F^2 p_y e\dot{A}}{\left(\Delta E^c_n\right)^2}\left(1 - \frac{q^2v_F^2}{\omega^2}\right)^{-3/2}. \tag{A8}$$

We can now immediately see that $\frac{d|c_n|^2}{du} = -\frac{d|c_{-n}|^2}{du}$, and since initial conditions are set to $c_m(u = -\infty) = 1$ and $c_{-m}(u = -\infty) = 0$, we obtain

$$|c_m(u)|^2 + |c_{-m}(u)|^2 = 1. \tag{A9}$$

APPENDIX B: NONLINEAR CURRENT RESPONSE

Let us find the Ψ_m contribution to the current density:

$$\begin{aligned} j_x &= e v_F \Psi^*_m\sigma_x\Psi_m \\ &= e v_F\sum_{n=\pm m}\left(|c_n|^2 d^*_n\sigma_x d_n + c^*_{-n}c_n e^{\frac{i}{\hbar}(S_n - S_{-n})}d^*_{-n}\sigma_x d_n\right). \end{aligned} \tag{B1}$$

From Eq. (A4) we can write the intraband matrix element:

$$d^*_n\sigma_x d_n = \frac{b_n^2}{L^2}n\cos\Phi_{\mathbf{P}^c_n - e\mathbf{A}} = \frac{b_n^2}{L^2}\frac{v^c_n}{v_F}, \tag{B2}$$

where we have introduced the classical velocity $v^c_n = \frac{\partial E^c_n}{\partial p^c_n} = n v_F\cos\Phi_{\mathbf{P}^c_n - e\mathbf{A}}$. Alternatively, using Eqs. (A5) and (A6) we can express the same matrix element as

$$\begin{aligned} d^*_n\sigma_x d_n &= n\frac{B_n^2}{L^2}\mathrm{Re}\left(D_n^2\right) = n\frac{B_n^2}{2L^2} \\ &\times\left(\frac{p_n - \frac{q}{\omega}E_n - eA}{\sqrt{\left(p_n - \frac{q}{\omega}E_n - eA\right)^2 + p_y^2\left(1 - \frac{q^2v_F^2}{\omega^2}\right)}} + n\frac{q v_F}{\omega}\right). \end{aligned} \tag{B3}$$

Next, using Eqs. (A5) and (A6), we can write the interband matrix element:

$$\begin{aligned} d^*_{-n}\sigma_x d_n &= -n\frac{B_n^2}{L^2}\,i\,\mathrm{Im}(D_{-n}D_n) \\ &= \frac{B_n^2}{2L^2}\frac{2iv_F p_y}{\Delta E^c_n}\left(1 - \frac{q^2v_F^2}{\omega^2}\right)^{-1/2}. \end{aligned} \tag{B4}$$

From Eqs. (A8) and (B4) we then obtain

$$\begin{aligned} &c^*_{-n}c_n e^{\frac{i}{\hbar}(S_n - S_{-n})}d^*_{-n}\sigma_x d_n + \text{c.c.} \\ &\quad = \frac{B_n^2}{2L^2}\frac{\Delta E^c_n}{v_F e\dot{A}}\left(1 - \frac{q^2v_F^2}{\omega^2}\right)\frac{d|c_{-n}|^2}{du}. \end{aligned} \tag{B5}$$

Finally, we can write the current density (B1) as

$$\begin{aligned} j_x = \frac{1}{L^2}\Bigg[&|c_m|^2 b_m^2 e v^c_m + |c_{-m}|^2 b^2_{-m} e v^c_{-m} \\ &+ \frac{\Delta E^c_m}{\dot{A}}\frac{B^2_m}{2}\left(1 - \frac{q^2v_F^2}{\omega^2}\right)\frac{d|c_{-m}|^2}{du}\Bigg]. \end{aligned} \tag{B6}$$

In the quasiclassical case of low frequencies interband transitions are exponentially suppressed, and we can approximately write $c_m \approx 1$, $c_{-m} \approx 0$, so that the current density

is $j_x = b_m^2 e v_m^c / L^2$. We note that this reduces to the classical single-band result $j_x^c = e v_m^c / L^2$ only in the nonlinear local case ($q = 0$) or in the linear nonlocal case. In other words b_m amounts to quantum nonlinear, nonlocal, interband correction. By using the density matrix it is straightforward to generalize this to the case of the electron Fermi sea described by the Fermi-Dirac distribution $f_m = \frac{1}{e^{(E_m - E_F)/kT}+1}$ as

$$j_x = \frac{4}{L^2}\sum_{p_m p_y} f_m b_m^2 e v_m^c = \frac{4}{h^2}\int dp_m dp_y\, f_m b_m^2 e v_m^c. \quad \text{(B7)}$$

By using Eqs. (B2) and (B3) we can write this in alternative form as

$$j_x = \frac{4ev_F}{h^2}\int dp_m dp_y\, f_m \frac{B_m^2}{2} m \times \left(\frac{p_m - \frac{q}{\omega}E_m - eA}{\sqrt{\left(p_m - \frac{q}{\omega}E_m - eA\right)^2 + p_y^2\left(1 - \frac{q^2 v_F^2}{\omega^2}\right)}} + m\frac{q v_F}{\omega} \right). \quad \text{(B8)}$$

The initial condition $b_m(u = -\infty) = 1$ requires that $B_m = \sqrt{\Delta E_m / E_m}$, where $\Delta E_m = E_m - E_{-m}$. From Eqs. (24) and (25) it is straightforward to show that

$$\frac{B_m^2}{2} = \frac{1 - m\frac{q v_F}{\omega}\frac{p_m}{\sqrt{p_m^2 + p_y^2}}}{1 - \frac{q^2 v_F^2}{\omega^2}}. \quad \text{(B9)}$$

Equation (B8) can then be rewritten in a more convenient form:

$$j_x = \frac{4e}{h^2}\int dp_1 dp_y\, f_1 \frac{\partial E_1^c}{\partial p_1} = -\frac{4e}{h^2}\int dp_1 dp_y \frac{\partial f_1}{\partial p_1} E_1^c, \quad \text{(B10)}$$

the last equation obtained by partial integration, and we assumed that we are dealing with the conduction band $m = 1$. Furthermore, in the low-temperature case $kT \ll E_F$ we can write $f_1 = \Theta(p_F - \sqrt{p_1^2 + p_y^2})$, so that $-\frac{\partial f_1}{\partial p_1} = \sum_s s\delta(p_1 - p_1^s)$, where $p_1^s = s\sqrt{p_F^2 - p_y^2}$ and $s = \pm 1$. We can then evaluate one integral from Eq. (B10) to obtain the current:

$$j_x = \frac{8ev_F}{h^2\left(1 - \frac{q^2 v_F^2}{\omega^2}\right)}\int_0^{p_F} dp_y \left[2\frac{q v_F}{\omega}\sqrt{p_F^2 - p_y^2} + \sqrt{\left(\sqrt{p_F^2 - p_y^2} - \frac{q v_F}{\omega}p_F - eA\right)^2 + p_y^2\left(1 - \frac{q^2 v_F^2}{\omega^2}\right)} - \sqrt{\left(-\sqrt{p_F^2 - p_y^2} - \frac{q v_F}{\omega}p_F - eA\right)^2 + p_y^2\left(1 - \frac{q^2 v_F^2}{\omega^2}\right)} \right]. \quad \text{(B11)}$$

APPENDIX C: LINEAR RESPONSE REGIME

For small fields $eA_0 \ll eA_{nl} = p_F(1 - \frac{q v_F}{\omega})$ we can linearize the current (B11) to obtain $j_x = i\omega\sigma(q,\omega)A$, where the conductivity $\sigma(q,\omega)$ can be evaluated explicitly:

$$\sigma(q,\omega) = \frac{i8\pi e^2 E_F \omega}{h^2 q^2 v_F^2}\left(\frac{1}{\sqrt{1 - \frac{q^2 v_F^2}{\omega^2}}} - 1 \right). \quad \text{(C1)}$$

Note that $\sigma(q,\omega)$ diverges as we approach the line $\omega = q v_F$, signaling the breakdown of linear response theory. This is also the reason why plasmon dispersion cannot cut this line [see Fig. 1(a)].

Note also that the oscillating current will induce the vector potential that will act back on the current. It is straightforward to solve Maxwell's equations for the current oscillating in the plane of graphene $j_x(\mathbf{r},t) = j_0 \sin(\omega t - qx)$ and show that it will induce a vector potential $A_x^{\text{ind}}(\mathbf{r},t) = A_0^{\text{ind}} \sin(\omega t - qx)$ of the amplitude

$$A_0^{\text{ind}} = \frac{-q j_0}{\omega^2 2\varepsilon_0 \varepsilon_r}, \quad \text{(C2)}$$

where $\varepsilon_r = (\varepsilon_{r_1} + \varepsilon_{r_2})/2$ is the average dielectric constant of materials surrounding graphene from above and below [12,32]. If we then introduce some external potential $A_x^{\text{ext}}(\mathbf{r},t) = A_0^{\text{ext}} \sin(\omega t - qx)$, the current will respond not only to A^{ext} but also to the total potential $A = A^{\text{ext}} + A^{\text{ind}} = A_0 \sin(\omega t - qx)$, i.e., $j_x = i\omega\sigma(q,\omega)A$. The amplitude of this self-consistent potential is then

$$A_0 = \frac{A_0^{\text{ext}}}{1 + \frac{iq\sigma(q,\omega)}{\omega 2\varepsilon_0 \varepsilon_r}}. \quad \text{(C3)}$$

One can see that it is possible to have self-sustained oscillations of the electron gas (plasmon-polaritons) even in the absence of the external field if $1 + \frac{iq\sigma(q,\omega)}{\omega 2\varepsilon_0\varepsilon_r} = 0$, with the corresponding plasmon dispersion

$$\omega(q) = q v_F \frac{ql + 1}{\sqrt{ql(ql + 2)}}, \quad \text{(C4)}$$

where we have introduced the length $l = \frac{\varepsilon_0 \varepsilon_r h^2 v_F}{4\pi e^2 p_F}$.

In the local case ($q = 0$) conductivity (C1) reduces to $\sigma(\omega) = \frac{i}{\omega}\frac{e^2 E_F}{\pi\hbar^2}$, in which case it is also easy to include losses (due to the impurity of phonon scattering) via the phenomenological damping rate γ as $\sigma(\omega) = \frac{i}{\omega + i\gamma}\frac{e^2 E_F}{\pi\hbar^2}$ [32]. It is usual to introduce the DC mobility μ via the relation $\sigma(0) = ne\mu$, so we can express the damping rate as $\gamma = \frac{e v_F^2}{\mu E_F}$.

APPENDIX D: LANDAU-ZENER MODEL

Let us focus on the state $\Psi_m(\mathbf{r},t) = \sum_n c_n(u)\Psi_n^{QC}(\mathbf{r},t)$, where $\Psi_n^{QC} = b_n \Psi_n^{qc}$ are our generalized quasiclassical states [Ψ_n^{qc} multiplied by $b_n(u)$ also satisfies the quasiclassical condition]. Now Ψ_n^{QC} are asymptotically exact solutions as long as we are far away from the transition point $E_n^c(u_0) = E_{-n}^c(u_0)$, which is generally complex [36]. We can then connect these asymptotic states by going into the complex u plane, always staying far away from the transition point u_0, so that the quasiclassicality condition is always satisfied. This way E_n^c from Eq. (20) simply changes the branch of the square root, i.e., turns into E_{-n}^c, with similar changes for other quantities. One can show that

$|c_{-m}(u=\infty)|^2 = \exp\left(\frac{1}{\hbar\omega}\mathrm{Im}\int_C \Delta E_m^c du\right) = K$, where the integration contour C goes around the transition point u_0 in the upper half plane for $m=-1$ and around u_0^* in the lower half plane for $m=1$ [36]. For convenience we write the energy gap explicitly:

$$\Delta E_m^c = E_m^c - E_{-m}^c = \frac{2mv_F}{1-\frac{q^2v_F^2}{\omega^2}}\sqrt{\left(p_m - \frac{q}{\omega}E_m - eA\right)^2 + p_y^2\left(1-\frac{q^2v_F^2}{\omega^2}\right)}, \tag{D1}$$

where we have used the fact that $p_{-m} - \frac{q}{\omega}E_{-m} = p_m - \frac{q}{\omega}E_m$. Generally, u_0 is complex, except in the case $p_y = 0$, where we can have real u_0 and a perfect transition $K=1$. This is completely analogous to the famous Klein tunneling in graphene where electrons can simply pass through the potential barrier by using the available negative-energy states [33]. Since K is the probability of transition into a different band during a single passage, then $1-K$ is the probability that an electron remains in the original band. As our field oscillates periodically in u, we also need to consider the transition probability for a double passage: $w = K(1-K) + (1-K)K = 2K(1-K)$ [36]. Finally, for very slow oscillations we can approximately say that the transition happens at a real point u where the gap $\Delta E_m^c(u)$ has a minimum since then the tunneling probability is largest. This generally happens at two points $\zeta < \xi$ during a single period, so we can write $|c_{-m}(u)|^2 \approx K\Theta(u-\zeta)\Theta(\xi-u) + 2K(1-K)\Theta(u-\xi)$, where $\Theta(u)$ is a step function. Of course, truncating dynamics to a single period only makes sense if $2K(1-K) \ll 1$, which is the only regime we explore in this paper. Finally, since $\frac{d\Theta(u)}{du} = \delta(u)$ is a δ function, we can write $\frac{d|c_{-m}(u)|^2}{du} = K\delta(u-\zeta) - K\delta(u-\xi) + 2K(1-K)\delta(u-\xi)$. When calculating dissipated power, the first two parts cancel, and the only term that contributes is

$$\frac{d|c_{-m}(u)|^2}{du} = 2K(1-K)\delta(u-\xi). \tag{D2}$$

[1] D. Cotter, R. J. Manning, K. J. Blow, A. D. Ellis, A. E. Kelly, D. Nesset, I. D. Phillips, A. J. Poustie, and D. C. Rogers, Nonlinear optics for high-speed digital information processing, Science **286**, 1523 (1999).

[2] K. S. Novoselov, D. Jiang, F. Schedin, T. J. Booth, V. V. Khotkevich, S. V. Morozov, and A. K. Geim, Two-dimensional atomic crystals, Proc. Natl. Acad. Sci. USA **102**, 10451 (2005).

[3] S. A. Mikhailov and K. Zeigler, Nonlinear electromagnetic response of graphene: Frequency multiplication and the self-consistent-field effects, J. Phys.: Condens. Matter **20**, 384204 (2008).

[4] E. G. Mishchenko, Dynamic Conductivity in Graphene beyond Linear Response, Phys. Rev. Lett. **103**, 246802 (2009).

[5] Q. Bao, H. Zhang, Y. Wang, Z. Ni, Y. Yan, Z. X. Shen, K. P. Loh, and D. Y. Tang, Atomic-layer graphene as a saturable absorber for ultrafast pulsed lasers, Adv. Funct. Mater. **19**, 3077 (2009).

[6] T. Oka and H. Aoki, Photovoltaic Hall effect in graphene, Phys. Rev. B **79**, 081406(R) (2009).

[7] K. L. Ishikawa, Nonlinear optical response of graphene in time domain, Phys. Rev. B **82**, 201402(R) (2010).

[8] M. M. Glazov, Second harmonic generation in graphene, JETP Lett. **93**, 366 (2011).

[9] H. Zhang, S. Virally, Q. Bao, L. K. Ping, S. Massar, N. Godbout, and P. Kockaert, Z-scan measurement of the nonlinear refractive index of graphene, Opt. Lett. **37**, 1856 (2012).

[10] M. Gullans, D. E. Chang, F. H. L. Koppens, F. J. García de Abajo, and M. D. Lukin, Single-Photon Nonlinear Optics with Graphene Plasmons, Phys. Rev. Lett. **111**, 247401 (2013).

[11] I. Al-Naib, J. E. Sipe, and M. M. Dignam, High harmonic generation in undoped graphene: Interplay of inter- and intraband dynamics, Phys. Rev. B **90**, 245423 (2014).

[12] M. Jablan and D. E. Chang, Multiplasmon Absorption in Graphene, Phys. Rev. Lett. **114**, 236801 (2015).

[13] F. Fillion-Gourdeau and S. MacLean, Time-dependent pair creation and the Schwinger mechanism in graphene, Phys. Rev. B **92**, 035401 (2015).

[14] M. M. Jadidi, J. C. König-Otto, S. Winner, A. B. Sushkov, H. D. Drew, T. E. Murphy, and M. Mittendorff, Nonlinear terahertz absorption of graphene plasmons, Nano Lett. **16**, 2734 (2016).

[15] Y. Wang, M. Tokman, and A. Belyanin, Second-order nonlinear optical response of graphene, Phys. Rev. B **94**, 195442 (2016).

[16] S. A. Mikhailov, Nonperturbative quasiclassical theory of the nonlinear electrodynamic response of graphene, Phys. Rev. B **95**, 085432 (2017).

[17] T. Higuchi, C. Heide, K. Ullmann, H. B. Weber, and P. Hommelhoff, Light-field-driven currents in graphene, Nature (London) **550**, 224 (2017).

[18] K. J. A. Ooi and D. T. H. Tan, Nonlinear graphene plasmonics, Proc. R. Soc. A **473**, 20170433 (2017).

[19] J. D. Cox, A. Marini, and F. J. García de Abajo, Plasmon-assisted high-harmonic generation in graphene, Nat. Commun. **8**, 14380 (2017).

[20] D. Dimitrovski, L. B. Madsen, and T. G. Pedersen, High-order harmonic generation from gapped graphene: Perturbative response and transition to nonperturbative regime, Phys. Rev. B **95**, 035405 (2017).

[21] M. Taucer, T. J. Hammond, P. B. Corkum, G. Vampa, C. Couture, N. Thiré, B. E. Schmidt, F. Légaré, H. Selvi, N. Unsuree, B. Hamilton, T. J. Echtermeyer, and M. A. Denecke, Nonperturbative harmonic generation in graphene from intense midinfrared pulsed light, Phys. Rev. B **96**, 195420 (2017).

[22] N. Yoshikawa, T. Tamaya, and K. Tanaka, High-harmonic generation in graphene enhanced by elliptically polarized light excitation, Science **356**, 736 (2017).

[23] H. A. Hafez, S. Kovalev, J. C. Deinert, Z. Mics, B. Green, N. Awari, M. Chen, S. Germanskiy, U. Lehnert, J. Teichert, Z. Wang, K. J. Tielrooij, Z. Liu, Z. Chen, A. Narita, K. Müllen, M. Bonn, M. Gensch, and D. Turchinovich, Extremely efficient terahertz high-harmonic generation in graphene by hot Dirac fermions, Nature (London) **561**, 507 (2018).

[24] B. Eliasson and C. S. Liu, Semiclassical fluid model of nonlinear plasmons in doped graphene, Phys. Plasmas **25**, 012105 (2018).
[25] Z. Sun, D. N. Basov, and M. M. Fogler, Universal linear and nonlinear electrodynamics of a Dirac fluid, Proc. Natl. Acad. Sci. USA **115**, 3285 (2018).
[26] T. Jiang, V. Kravtsov, M. Tokman, A. Belyanin, and M. B. Raschke, Ultrafast coherent nonlinear nanooptics and nanoimaging of graphene, Nat. Nanotechnol. **14**, 838 (2019).
[27] C. J. Tollerton, J. Bohn, T. J. Constant, S. A. R. Horsley, D. E. Chang, E. Hendry, and D. Z. Li, Origins of all-optical generation of plasmons in graphene, Sci. Rep. **9**, 3267 (2019).
[28] A. Principi, D. Bandurin, H. Rostami, and M. Polini, Pseudo-Euler equations from nonlinear optics: Plasmon-assisted photodetection beyond hydrodynamics, Phys. Rev. B **99**, 075410 (2019).
[29] J. D. Cox and F. J. García de Abajo, Nonlinear graphene nanoplasmonics, Acc. Chem. Res. **52**, 2536 (2019).
[30] P. A. D. Gonçalves, N. Stenger, J. D. Cox, N. A. Mortensen, and S. Xiao, Strong light-matter interactions enabled by polaritons in atomically thin materials, Adv. Opt. Mater., 1901473 (2020).
[31] M. Tonouchi, Cutting-edge terahertz technology, Nat. Photonics **1**, 97 (2007).
[32] M. Jablan, H. Buljan, and M. Soljačić, Plasmonics in graphene at infrared frequencies, Phys. Rev. B **80**, 245435 (2009).
[33] M. I. Katsnelson, K. S. Novoselov, and A. K. Geim, Chiral tunneling and the Klein paradox in graphene, Nat. Phys. **2**, 620 (2006).
[34] A. H. Castro Neto, F. Guinea, N. M. R. Peres, K. S. Novoselov, and A. K. Geim, The electronic properties of graphene, Rev. Mod. Phys. **81**, 109 (2009).
[35] D. M. Volkov, Concerning a class of solutions of the dirac equation, Z. Phys. **94**, 250 (1935).
[36] L. D. Landau and E. M. Lifshitz, *Quantum Mechanics*, 3rd ed. (Butterworth-Heinemann, Amsterdam, 2003).
[37] L. D. Landau and E. M. Lifshitz, *Mechanics*, 3rd ed. (Butterworth-Heinemann, Amsterdam, 2007).
[38] L. D. Landau and E. M. Lifshitz, *The Classical Theory of Fields*, 4th revised English ed. (Butterworth-Heinemann, Amsterdam, 2009).
[39] L. D. Landau and E. M. Lifshitz, *Statistical Physics*, 3rd ed. (Butterworth-Heinemann, Amsterdam, 2010), Part 1.
[40] L. V. Keldysh, Ionization in the field of a strong electromagnetic wave, Zh. Eksp. Teor. Fiz. **47**, 1945 (1964) [Sov. Phys. JETP **20**, 1307 (1965)].
[41] E. H. Hwang and S. Das Sarma, Acoustic phonon scattering limited carrier mobility in two-dimensional extrinsic graphene, Phys. Rev. B **77**, 115449 (2008).
[42] K. I. Bolotin, K. J. Sikes, J. Hone, H. L. Stormer, and P. Kim, Temperature-Dependent Transport in Suspended Graphene, Phys. Rev. Lett. **101**, 096802 (2008).
[43] L. D. Landau, E. M. Lifshitz, and L. P. Pitaevskii, *Electrodynamics of Continuous Media*, 2nd ed. (Butterworth-Heinemann, Amsterdam, 2007).
[44] C. Mouhot and C. Villani, On Landau damping, Acta Math. **207**, 29 (2011).
[45] P. B. Corkum, Plasma Perspective on Strong Field Multiphoton Ionization, Phys. Rev. Lett. **71**, 1994 (1993).
[46] M. Lewenstein, Ph. Balcou, M. Yu. Ivanov, A. L'Hullier, and P. B. Corkum, Theory of high-harmonic generation by low-frequency laser fields, Phys. Rev. A **49**, 2117 (1994).
[47] P. Antoine, A. L'Hullier, and M. Lewenstein, Attosecond Pulse Trains Using High-Order Harmonics, Phys. Rev. Lett. **77**, 1234 (1996).